The International Journal of Advanced Manufacturing Technology (2022) 120:7755–7770
https://doi.org/10.1007/s00170-022-09265-2

ORIGINAL ARTICLE

Energy consumption modeling of additive-subtractive hybrid manufacturing based on cladding head moving state and deposition efficiency

Wen Liu[1,2] · Haiying Wei[1,2] · Min Zhang[1,2] · Yaoen Luo[1,2] · Yi Zhang[1,2]

Received: 21 October 2021 / Accepted: 23 April 2022 / Published online: 4 May 2022

Abstract

Additive-subtractive hybrid manufacturing (ASHM) process consumes a large amount of electrical energy during the processing stage due to the low process rate and high energy density. A reliable prediction of energy consumption is the starting point to develop potential energy-saving strategies. However, the power consumption characteristics of ASHM system are dynamic due to the non-continuous moving path and non-uniform moving speed of the cladding head. Besides, the cutting allowance of each sub-cutting process is fragmented and hard to be obtained because of the multiple alternate characteristics of the additive manufacturing (AM) and subtractive manufacturing (SM) during the processing stage. This paper proposed a combined energy consumption model based on process characteristics, which consists of a state-based AM energy consumption model and a cutting allowance-based SM energy consumption model. At AM stage, the energy consumption is classified into the deposition energy consumption, rapid moving energy consumption, and pause energy consumption based on the cladding head moving state. The power in each moving state is identified by the working statuses of machine sub-systems, and the duration is related to the length of moving path, number of inflection points, as well as the scanning speed. At SM stage, the deposition efficiency was introduced to characterize the volume fraction of total cutting allowance for machining the deposited part, and the energy consumption model is extrapolated as a function of the deposition efficiency and specific energy consumption (SEC). Experimental results show that the model could offer the prediction of energy consumption with an accuracy of more than 97%, and the breakdown analysis demonstrated that the AM energy consumption accounts for more than 80% of the whole ASHM energy consumption. It is recommended to increase the scanning speed and process rate under the premise of ensuring good forming quality to reduce the total ASHM energy consumption.

Keywords Additive-subtractive hybrid manufacturing · Energy consumption · Modeling · Moving state · Deposition efficiency

Abbreviations

AM	Additive manufacturing
SM	Subtractive manufacturing
ASHM	Additive-subtractive hybrid manufacturing
LDED	Laser-directed energy deposition
SLM	Selective laser melting
SLS	Selective laser sintering
FDM	Fused deposition modeling

List of symbols

E_{total}	The total energy consumption of ASHM process (MJ)
$E_{additive}$	The energy consumption of AM process (MJ)
$E_{subtractive}$	The energy consumption of SM process (MJ)
$E_{exchange\_up}$	The energy consumption when the cladding head replaces cutting tool (MJ)
$E_{exchange\_down}$	The energy consumption when the cutting tool replaces cladding head (MJ)
$E_{deposition}$	The energy consumption of deposition state in AM (MJ)

✉ Haiying Wei
why@hnu.edu.cn

1 State Key Laboratory of Advanced Design and Manufacturing for Vehicle Body, Hunan University, Changsha 410082, People's Republic of China

2 Key Laboratory for Intelligent Laser Manufacturing of Hunan Province, Hunan University, Changsha 410082, People's Republic of China

E_{rapid}	The energy consumption of rapid moving state in AM (MJ)
E_{pause}	The energy consumption of pause state in AM (MJ)
$P_{standby\_mahcine\ tool}$	The standby power of machine tool (W)
$P_{standby\_laser}$	The standby power of laser machine (W)
$P_{standby\_chiller}$	The standby power of laser chiller machine (W)
P_{powder}	The power required to drive the stepping motor of powder feeder (W)
$P_{working\_laser}$	The power required to emit the laser beam (W)
$P_{working\_chiller}$	The power required to drive the fan of laser chiller machine (W)
P_{feed}	The feed power of machine tool (W)
P_{fast_feed}	The fast feed power of machine tool (W)
m_{ASHM}	The mass of the ASHM part (g)
$m_{depositon}$	The mass of the deposited part (g)
$L_{deposition}$	The length of the deposition path (mm)
$L_{rapid\ moving}$	The length of the rapid moving path (mm)
$t_{deposition}$	The time in deposition state (s)
t_{rapid}	The time in rapid moving state (s)
Δt_{pause}	The duration of each pause (s)
n_{pause}	The number of pauses
N_{up}	The number of up exchange process
N_{down}	The number of down exchange process
$k_{chiller}$	The ratio of the deposition time to the working time of chiller fan
P_{output}	The laser output power (W)
v_s	The scanning speed (mm/min)
v_f	The powder feed rate (g/min)
ρ_{mat}	The material density (g/mm^3)
$\eta_{deposition}$	The deposition efficiency (%)
MRR	The material removal rate in SM (mm^3/min)
PR	The process rate in AM (g/min)
SEC	Specific energy consumption (J/mm^3)
SPE	Specific printing energy (MJ/kg)

1 Introduction

Additive-subtractive hybrid manufacturing (ASHM) is a process that synergistically integrates additive and subtractive processes within a single workstation [1, 2]. This technique takes advantage of the near-net shaping of additive manufacturing (AM) and the attainable accuracy of subtractive manufacturing (SM), which has been applied to the manufacture of internal, overhanging, and high-aspect-ratio feature components with expected geometric accuracy and surface roughness, such as molds, aircraft engines, and aerospace brackets [3–5]. The concept of combining laser-directed energy deposition (LDED) and CNC milling within a highly mobile multi-axis machine tool is a common type of ASHM process [6, 7]. The most remarkable feature is that it can realize the real-time alternate operation of AM and SM during processing stage, as shown in Fig. 1. Three promising advantages stand out: (1) the SM process can be carried out before cavity closure or cutting interference; (2) the positioning errors can be avoided due to one-time clamping; and (3) the scheduling time can be saved due to the rapid alternation of additive and subtractive processes.

However, the recent studies showed that the energy-efficient manufacturing of ASHM process could not always achieved due to the huge electrical energy consumption at AM stage. According to the report provided by Gutowski et al. [8], the average specific printing energy (SPE) of additive processes is about 1 to 2 orders of magnitude higher than conventional manufacturing processes, while the process rate (PR) is about 3 orders of magnitude smaller than conventional processes. Kellens et al. [9] also claimed that the specific energy values for AM unit processes are 1 to 2 orders of magnitude higher compared to conventional machining and injection molding processes. Therefore, the research on energy-saving strategies for ASHM process has become a hot topic when facing the dual pressure of substantially deteriorating environment and constantly increasing energy costs in recent years. Developing the energy consumption model for ASHM process is essential for energy-saving. Well-designed energy consumption model could not only provide the knowledge of the energy consumption of each energy-consuming sub-component, but also help to

Fig. 1 The schematic description of ASHM process

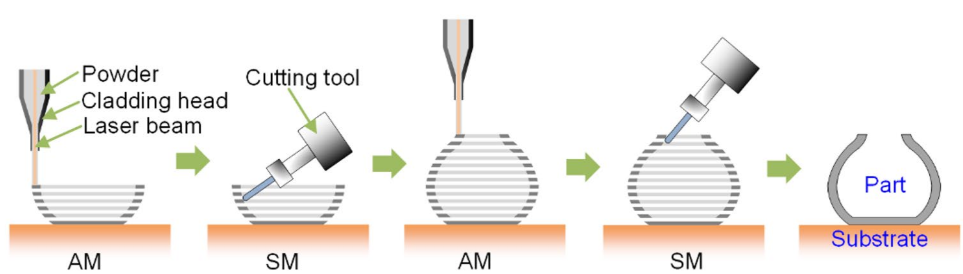

realize the precise simulations with respect to various process parameters [10].

Generally, the energy consumption is obtained by the product of SPE and mass of the part. Some researchers prefer to use the fixed SPE data and apply it to the life cycle assessment [11–13]. Nevertheless, there are considerable differences in SPE when the AM process is different or the process parameters and materials are varied with the same AM process. For example, the SPE varies from 32.3 to 7708 MJ/kg, a difference of two orders of magnitude [14]. In addition, other researchers have been devoted to modeling the energy consumption for selective laser melting/sintering (i.e., SLM/SLS, a type of AM technology) process. Peng and Chen [15] developed a stage-based energy consumption model for SLM process, which considering the preparation, building, and finishing stages. Lv et al. [16] proposed a novel method to forecast the energy consumption of SLM process based the power modeling of machine subsystems and the temporal modeling of sub-processes, and the prediction accuracy is more than 84%. Feng et al. [17] divided the total energy consumption of SLS process into several energy consumption systems, including the high power laser system, heating insulation system, powder delivery system, and auxiliary systems, and applied the model to conduct the synergistic optimization of energy consumption and material costs. However, the LDED process has a completely different processing flow compared with SLM process. For example, the SLM process includes the steps of pumping out air, filling with inert gas, powder layering, laser scanning parts, supports and so on, while the LDED process is accomplished by simultaneously delivering the metallic powder and focused laser energy with the moving cladding head [18, 19]. There must be a pertinent energy consumption model based on the process characteristics of LDED process to achieve the accurate prediction of energy consumption.

The non-continuous moving path and non-uniform moving speed of cladding head are the most significant characteristics of LDED process, which leads to the increased time and resultant energy consumption. On the one hand, the cladding head needs to be repositioned to continue filling in another region, which may lead to increased idle time in traveling the useless linking paths [20–22]. On the other hand, the deposition speed has a sudden change among the corner of deposition path, and the resultant acceleration and deceleration process will extend the deposition time [23]. In brief, the deposition process is frequently interrupted by factors of toolpath changes, tool start-stop and non-deposition time, which will result in spending more total manufacturing time and the associated energy consumption [24]. Komineas et al. [25] pointed out that the total manufacturing time is composed of deposition time and rapid moving time in the fused deposition modeling (FDM) process. However, in LDED process, the cladding head moving state includes deposition state, rapid moving state, and pause state. At the pause state, the cladding head is stationary at the inflection point from start-to-stop or stop-to-start, and the laser beam is correspondingly in the pre-open or pre-closed state to avoid the accumulation of excess melted material at the inflection point [26]. There is a time delay between the opening and closing of the laser beam. Generally, a complex part involves thousands of inflection points, which may produce a considerable time error when the pause state is not considered. Therefore, the energy consumption of pause state and the impact on the overall energy consumption need to be further studied.

Furthermore, the manufacturing of a complex structure by using ASHM process requires multiple alternations between AM and SM process [27], and the processing stage of "deposition - milling" presents non-continuous characteristics, which makes it hard to obtain the fragmented cutting allowance of each sub-SM process. Generally, the electrical energy consumption is modeled as the integration of power consumption in time [28]. However, the power consumptions from different stages vary greatly due to the varied processing conditions [29, 30]. Besides, the planned path length is not proportional to time [31]. The feed axis has a short dwell time at the inflection point, and the speed changes abruptly [23]. The discrete sub-cutting process, the variation in the number of inflection points caused by path planning, and the acceleration and deceleration of the feed axis at the inflection point lead to the difficulty in accurately predicting manufacturing time [32–34]. In order to reduce the complexity of energy consumption prediction, the calculation of time and energy consumption for each sub-SM process must be avoided. How to find a correlation factor to relate the SM energy consumption, total cutting allowance, and deposition volume of the manufactured complex structure for modeling the energy consumption of ASHM process is particularly important.

This paper proposed an energy consumption model for ASHM process based on cladding head moving state and total cutting allowance to accurately predict the energy consumption and perform the breakdown analysis to support the appropriate energy-saving solutions. First, the AM energy consumption is classified into the deposition energy consumption, rapid moving energy consumption, and pause energy consumption based on the cladding head moving state, and a state-based energy consumption model was proposed for LDED process. Then, the deposition efficiency was introduced to characterize the volume fraction of total cutting allowance for a given part, and the SM energy consumption is associated with the deposition efficiency and specific energy consumption (SEC). Finally, the comparison model was tested on two experimental studies. The first one concerns the different scanning strategies on the AM energy consumption results, and the second one concerns the process parameters on the effect of total ASHM energy consumption. The purposed method provided a basic for the energy prediction and energy-saving research of ASHM process.

This paper is organized as follows: In Sect. 2, the energy consumption characteristics and classification of ASHM process were elaborated, and the deposition efficiency was introduced. In Sect. 3, a combined energy consumption model was developed. In Sect. 4, the experimental design and setup and coefficients calibration of power models for ASHM machines were described. In Sect. 5, the model verification and comparison, the energy consumption breakdown analysis, and the energy-saving suggestions were presented. In Sect. 6, the conclusions were provided.

2 Methodology

2.1 Energy consumption characteristics and classification

A schematic description of the ASHM process is illustrated in Fig. 2. At AM stage, the cladding head, which consists of either a single or multiple powder-spray nozzles, is moved along with the deposition path. The laser beam provides sufficient thermal energy to melt the ejected particles to form the near-net parts layer by layer. At SM stage, the milling process is applied to achieve the desirable geometrical accuracy and surface quality. Additive and subtractive processes can be alternated within a single workstation during processing stage, which avoids the error caused by secondary clamping and achieves the rapid manufacture of complex parts that cannot be machined at all in conventional milling process due to the accessibility constraint (Fig. 2a).

Figure 2b shows the corresponding power consumption during ASHM process. According to the whole operations of ASHM process when manufacturing the final part, the energy consumption can be classified into AM energy consumption, SM energy consumption, and exchange energy consumption. At each stage, its power consumption is different due to different energy-consuming equipment participating in the work. For example, the machine tool is used to provide feed movement of cladding head at AM stage and conduct milling process at SM stage. The laser machine is used for exporting laser energy to melt metal powder particles at AM stage. The laser chiller machine is served to cool laser machine and cladding head, and the powder feeder is used to transfer metal powder particles to cladding head at AM stage. The power of each equipment is complicated and dynamic, which is closely relevant with the process parameters, such as laser power, scanning speed and powder feeding rate, etc.

The AM energy consumption is related to the deposition path and process parameters. Different scanning strategy or process parameters may lead to the differences in the deposition length, rapid moving length and the number of pauses, and finally the differences of the deposition time. The SM energy consumption is related to the cutting allowance and

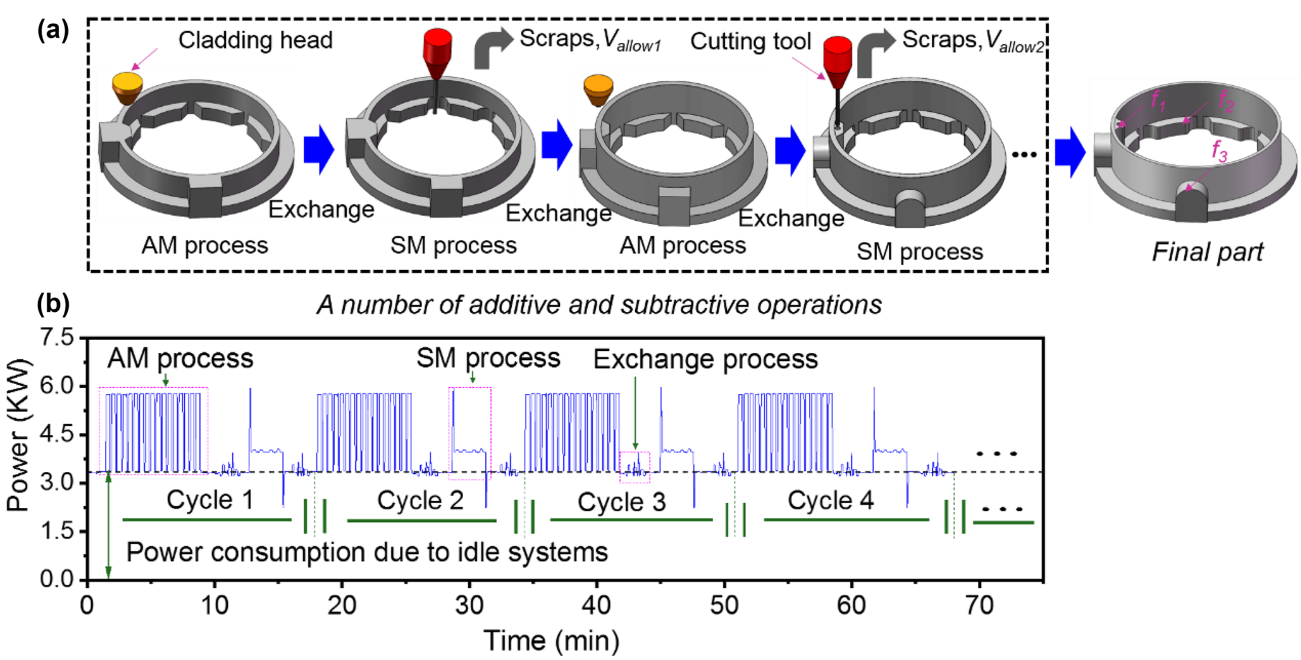

Fig. 2 Example for manufacturing the simplified bearing bracket by ASHM process: (**a**) the process steps; (**b**) the corresponding power consumption

cutting parameters. Different from the conventional SM process, the unused equipment at SM stage, such as laser machine, laser chiller machine, and powder feeder machine, should be in standby mode to prepare for the immediate start of AM process, which will consume a large number of electrical energy. In the exchange process, there are two sub-processes: cutting tool replaces cladding head when AM process is finished and cladding head replaces cutting tool when SM process is finished. Both of the two sub-processes contain a variety of motion processes, including feed axis movement in x/y/z directions, motor rotation of cutting tool library, and motor rotation of cladding head support frame. Each process spends different time and energy; therefore, the exchange energy consumption can be split into up exchange energy consumption (cladding head replaces cutting tool) and down exchange energy consumption (cutting tool replaces cladding head).

2.2 Cladding head moving state on energy consumption at AM stage

During deposition, the cladding head presents a non-continuous and non-uniform moving state, as shown in Fig. 3. At step "a–b," the cladding head moves continuously, and the laser machine emits laser to melt the powder material to form a track. After reaching the inflection point, as presented in step "b–c," the cladding head switches from the moving state to the static state, accompanied by the laser machine from the on-to-off state. At step "c–d," the cladding head moves rapidly to travel the offset distance between the tracks, and the laser machine is in the off state to avoid the accumulation of excess melted material at the inflection point [26]. At step "d–e," the cladding head stops again, and the laser machine is in the off-to-on state to prepare for the next cycle of the deposition. There is a time delay regardless of whether the laser machine is in the on-to-off or off-to-on state. The operation state of laser machine follows the moving state of cladding head, which leads to the change of power consumption at AM stage. Since there are thousands or even tens of thousands of inflection points in the deposition of a complex part, the energy consumption of AM stage in pause state at the inflection point cannot be ignored. Therefore, according to the moving state of the cladding head, the AM energy consumption can be further classified into deposition energy consumption, rapid moving energy consumption, and pause energy consumption, as listed in Table 1.

2.3 Energy consumption of SM stage related to deposition efficiency

The as-deposited part must reserve enough cutting allowance to ensure the good surface integrity for the followed SM process. A complex structure is usually subjected to multiple "deposition-milling" sequential processing stages, which can lead to discrete cutting allowances and the resultant fragmented SM energy consumption (Fig. 2). The total energy consumption at SM stage is then composed of the energy consumption of multiple sub-SM processes. At each sub-SM process, the energy consumption can be obtained by the product of cutting allowance and

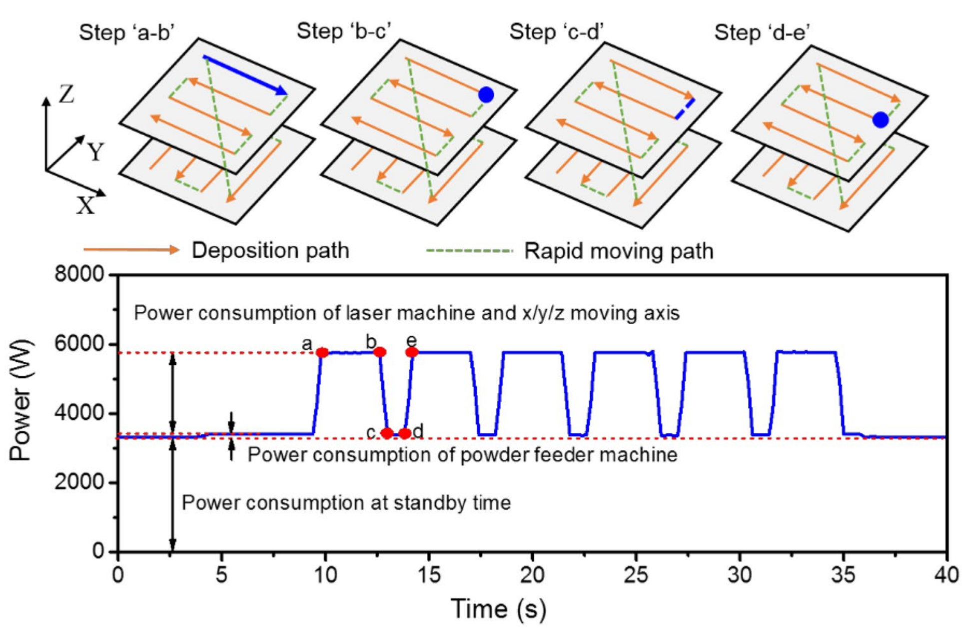

Fig. 3 Cladding head moving state and corresponding power consumption profile

Table 1 Energy consumption classification at AM stage

Items	Definition	Power consumption characteristics
Deposition energy consumption	Energy consumption when the cladding head moves at a constant speed and the laser machine is in the on state	The total power is the sum of laser machine working power, cladding head moving power, powder feeder power and standby power; The duration is related to the deposition path and the scanning speed
Rapid moving energy consumption	Energy consumption when the cladding head moves rapidly and the laser machine is in the off state	The power includes the cladding head moving power, powder feeder power and standby power; The duration is related to the rapid moving path and the rapid moving speed
Pause energy consumption	Energy consumption when the cladding head at start-to-stop or stop-to-start inflection points	The power is related to the laser machine working power and standby power; The duration is related to the number of pauses

specific energy consumption. Therefore, the total energy consumption of SM stage is presented in Eq. (1).

$$E_{subtractive} = V_{allow1} \cdot SEC_1 + V_{allow2} \cdot SEC_2 + \cdots + V_{allow\,n} \cdot SEC_n = \sum_{i=1}^{n} V_{allow\,i} \cdot SEC_i \quad (1)$$

In order to avoid the calculation of cutting allowance for each sub-SM process, considering the total cutting allowance of multiple cuts will greatly reduce the difficulty in energy consumption prediction. From the perspective of the entire ASHM process, the total cutting allowance is approximately equal to the total deposition volume minus the volume of final part.

$$\sum_{i=1}^{n} V_{allow\,i} \approx V_{deposition} - V_{ASHM} \quad (2)$$

The deposition efficiency, used to characterize material waste extent and forming quality in AM process [35], is introduced here to intuitively describe the material utilization rate in ASHM. It was defined as the ratio of final volume of the part to the deposited volume of the part (Fig. 2a).

$$\eta_{deposition} = \frac{V_{ASHM}}{V_{deposition}} \cdot 100\% \quad (3)$$

During ASHM process, the cutting process parameters of each sub-SM stage such as cutting depth, cutting width, and feed rate are set at optimized levels in order to achieve a low surface roughness. Usually, the process parameters are maintained constant at each sub-SM process to obtain consistent surface roughness, and the SEC data can be considered to be approximately the same in the case of the same cutting material, process parameters, and machine tool equipment. Therefore, Eq. (1) can be simplified as:

$$E_{subtractive} = \sum_{i=1}^{n} V_{allow\,i} \cdot SEC \quad (4)$$

Substituting Eqs. (2) and (3) into Eq. (4):

$$E_{subtractive} = SEC \cdot V_{deposition}\left(1 - \eta_{deposition}\right) \quad (5)$$

Both of the volume of the final ASHM part and deposited AM part can be obtained from 3D data at the design stage. Different cutting allowances lead to different deposition efficiencies, which affects the cutting energy consumption of SM stage. Therefore, the cutting energy consumption of SM stage cannot be regarded as a fixed value for different parts, it is closely related to the deposition efficiency.

3 Energy consumption modeling for ASHM process

According to the classification of ASHM process, the total energy consumption is composed of AM energy consumption, SM energy consumption, and exchange energy consumption.

$$E_{total} = E_{additive} + E_{subtractive} + E_{exchange} \tag{6}$$

At AM stage, the energy consumption can be classified into deposition energy consumption, rapid moving energy consumption and pause energy consumption, as presented in Eq. (7). All of them include standby energy consumption. The standby energy consumption is used to activate energy-consuming components to ensure the machine is ready for working. The power of involved equipment is independent of process parameters, and the energy consumption is only time dependent. The standby power is composed of the standby power of machine tool, laser machine, laser chiller machine, and powder feeder. Except the standby energy consumption, deposition energy consumption also includes laser working energy consumption, powder feeder energy consumption, feed axis movement energy consumption of machine tool, and fan working energy consumption of laser chiller machine. Their power values are decided by process parameters.

$$\begin{cases} E_{additive} = E_{deposition} + E_{rapid} + E_{pause} \\ E_{deposition} = \left(P_{standby} + P_{powder} + P_{working\_laser} + \frac{1}{K_{chiller}} \cdot P_{working\_chiller} + P_{feed}\right) \cdot t_{deposition} \\ E_{rapid} = \left(P_{standby} + P_{powder} + P_{fast\_feed}\right) \cdot t_{rapid} \\ E_{pause} = \left(P_{standby} + P_{powder} + 0.5 \cdot P_{working\_laser}\right) \cdot \Delta t_{pause} \cdot n_{pause} \end{cases} \tag{7}$$

At SM stage, the energy consumption can be predicted by cutting volume and specific energy consumption (SEC). The cutting volume is related to the deposition efficiency, while the SEC can be correlated with the material removal rate (MRR), by applying the empirical method proposed by Kara and Li [36], as presented in Eq. (8).

$$\begin{cases} E_{subtractive} = SEC \cdot V_{deposition}\left(1 - \eta_{deposition}\right) \\ SEC = C_0 + \frac{C_1}{MRR} \end{cases} \tag{8}$$

At exchange stage, there are two sub-processes, namely up exchange process and down exchange process, as claimed in Sect. 2.1. The number indicators (N_{up}, N_{down}) are introduced to characterize the energy consumption of the two processes:

$$E_{exchange} = \left[E_{exchange\_up} \;\; E_{exchange\_down} \right] \begin{bmatrix} N_{up} \\ N_{down} \end{bmatrix} \tag{9}$$

The total energy consumption of ASHM process for producing a specific part can be predicted from the energy model as presented in Eqs. (6), (7), (8), and (9). Table 2 shows the explanation and modeling for each power and time consumption.

The ASHM machine tool is controlled by numerical control (NC) codes. These NC codes are linked to a series of movement of machine tool components, such as axis feed, spindle, worktable, and tool change system. After the scanning path is generated by the trajectory planning, the relevant information such as the length of deposition path, rapid moving path, and number of inflection points can be extracted from the NC codes. Table 3 summarizes the common NC codes as related to machine components and their operations. The energy consumption can be estimated by the developed model based on the machine tool energy state equations that can be related to the NC codes.

4 Experiments

4.1 Experimental design

In order to verify the accuracy of the ASHM energy consumption model and explore the impact of process parameters and deposition efficiency on the total energy consumption, two exploration experiments were proposed as follows, and the 316L material was used for experimental analysis (the density of 316L material is 7.98 g/cm^3). The corresponding variable settings are shown in Table 4.

- ***Test 1***
  Exploring the impact of scanning strategy on total energy consumption, obtaining the energy consumption proportion of cladding head under different motion states at AM stage, and providing ideas for energy-saving. The test was designed by using four scanning strategies, namely, "identical," "orthogonal," "outer perimeter + orthogonal," and "contour." For the same part, different scanning strategies affect the length of deposition path, rapid moving path, and number of inflection points, which ultimately affects the energy consumption of AM stage. The four kinds of scanning strategies are illustrated in Fig. 4.
- ***Test 2***
  Exploring the variation of deposition efficiency under different AM process parameters, as well as the

Table 2 Explanation and modeling for each power and time consumption

Symbols	Explanation	Modeling
$P_{standby}$	$P_{standby}$ is the sum of the standby power of machine tool, laser machine, laser chiller machine, and powder feeder. All of these equipment are switched ON but without working	$E_{standby} = P_{standby\_machine\ tool} + P_{standby\_laser} \cdots$ $+ P_{standby\_chiller} + P_{standby\_powder\ feeder}$ where $P_{standby\_machine\ tool}$ is the standby power of machine tool; $P_{standby\_laser}$ is the standby power of laser machine; $P_{standby\_chiller}$ is the standby power of chiller machine; $P_{standby\_powder\ feeder}$ is the standby power of powder feeder
P_{powder}	P_{powder} is the power required to convey the powder particles. The faster the stepping motor in the powder feeder, the higher the powder feed rate. Thus the power has a linear relationship with powder feed rate	$P_{powder} = k_{powder} \cdot v_f + b_{powder}$ where v_f is the powder feed rate. k_{powder} and b_{powder} are the coefficients
$P_{working\_laser}$	$P_{working\_laser}$ is the power consumption used for depositing a desired part. It happens when the laser machine delivers the laser power. The laser working power value has a linear relationship with laser output power	$P_{working\_laser} = k_{laser} \cdot P_{output} + b_{laser}$ where P_{output} is the laser output power, which is one of the most important process parameters in AM process. k_{laser} and b_{laser} are the coefficients
$P_{working\_chiller}$	$P_{working\_chiller}$ is the power required to drive the fan of laser chiller machine. The fan is working in the deposition phase and governed by water temperature; when the temperature exceeds the high temperature setting value, the fan will rotate to lower the water temperature; when the water temperature drops to a low temperature setting, the fan stops turning. It has periodicity	$P_{working\_chiller}$ is approximately a constant value, $k_{chiller}$ is the coefficient of the deposition time to the working time of fan
P_{feed}	P_{feed} is the working power of the CNC hybrid machine tool. It is the power required to move the spindle when depositing a desired part	$P_{feed} = k_0 + k_1 \cdot v_s + k_2 \cdot v_s^2$ where k_0, k_1, and k_2 are the coefficients about the power and scanning speed (v_s) of spindle movement
$t_{deposition}$	$t_{deposition}$ is the duration when the cladding head is in the deposition state. It is related to deposition path and scanning speed	$t_{deposition} = L_{deposition} / v_s$ where $L_{deposition}$ is the deposition length
t_{rapid}	t_{rapid} is the duration when the cladding head is in the rapid moving state. It is related to rapid moving path and fast moving speed	$t_{rapid} = L_{rapid} / v_{fast\_feed}$ where L_{rapid} is the rapid moving length, v_{fast_feed} is the rapid feed rate
Δt_{pause}	Δt_{pause} is the delay time when the cladding head is in start-stop state or stop-start state	Δt_{pause} is a constant value, approximately 0.4 s

Table 3 Relationship between NC code of AM stage and energy consumption on ASHM system

NC code	Machine components	CNC codes	Operations at AM stage
G-code	X, Y, Z axis	G00	Rapid move
		G01	Linear motion with defined feed rate
		G02,G03	Circular interpolation
F-code	X, Y, Z axis	F	Defined feed rate
M-code	Laser machine	M10	Laser program start
		M11	Laser program off
	Powder feeder	M50, M52	Powder feeder start
		M51, M53	Powder feeder off
Semantic code	Laser shutter	LASER_ON	Turn on laser beam
		LASER_OFF	Turn off laser beam

influence of deposition efficiency on cutting energy consumption at SM stage. The *D2 path* was used as the scanning strategy. The laser output power and scanning speed were set as variables, while the optimized linear energy density (i.e., laser output power divided by scanning speed) of 60 J/mm in AM was adopted based on a series of preliminary experiments. The other process parameters are constant.

Both of the two tests were applied to the manufacture of the same block parts with the dimensional size of 36 mm × 36 mm × 8 mm in terms of length, width, and height. The relevant data of the four scanning strategies (Fig. 4) are shown in Table 5. When the AM process finished, the SM process was carried on to remove the allowance of the sample. In SM process, the tool path for both face milling and flank milling were selected as zigzag cutting pattern.

4.2 Experimental setup

The experimental apparatus of ASHM process is shown in Fig. 5. The ASHM system consists primarily of a laser generation system, a CNC hybrid machine tool system, a powder delivery system, and a cooling system (i.e., laser chiller machine). A high power fiber laser with a beam wavelength of 1070 ± 10 nm (YLS-5000, IPG) was used to melt coaxially delivered powders on to the substrate for parts production. The CNC hybrid machine tool was jointly developed by Hunan University and Han's Laser, which can realize the function of additive and subtractive hybrid manufacturing. Its associated components consist of a laser cladding head with four coaxial nozzles and a tool magazine for milling process. The powder feeder (DPSF-2) has two chambers, which can achieve the printing of multiple materials to fabricate functional gradient parts. Argon was used as shielding gas and delivering gas. Cemented carbide tools (SECO) with diameter of 16 mm and 3 teeth were used in cutting process. Total energy consumption of all involved machines was measured on bus by using a HIOKI power analyzer (PQ3100).

4.3 Power calibration of machines

According to the analysis in Sect. 3, the power in each machine has both constant values and variable values along with process parameters. The constant power which measured by HIOKI power analyzer are shown in Table 6.

Table 4 Process parameters in ASHM

Tests	Samples	Process parameters at AM stage						Process parameters at SM stage	
		Laser output power (W)	Scanning speed (mm/min)	Powder feed rate (g/min)	Layer thickness (mm)	Hatch spacing (mm)	Process rate[a] (g/min)	MRR (mm^3/min)	Deposition efficiency (%)
Test 1	D1–D4	700	700	8.6	0.2	1.2	1.34	-	-
Test 2	S1	500	500	8.6	0.2	1.2	0.96	153	80
	S2	700	700	8.6	0.2	1.2	1.34		78
	S3	900	900	8.6	0.2	1.2	1.72		76
	S4	1100	1100	8.6	0.2	1.2	2.11		73

[a]Process rate = layer thickness × hatch spacing × scanning speed × material density

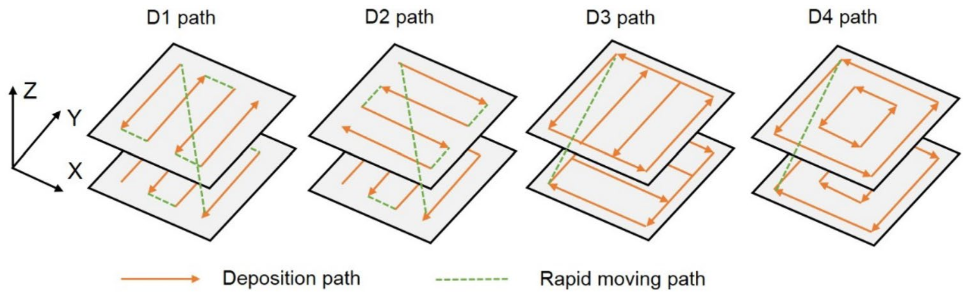

Fig. 4 Four kinds of scanning strategies at AM stage (D1, identical; D2, orthogonal; D3, outer perimeter + orthogonal; D4, contour)

Figure 6 shows the power of machines at different process parameters. Table 7 presents the specific fitting relation formula of process parameters and power consumption. It can be summarized that the fitting degree of all the relation formulas is over 0.9. Therefore, the fitting model can be used to predict the energy consumption in ASHM process.

Since the time of the exchange process and tool change process are constant, it can be simplified as a fixed energy consumption. Through three experimental measurements, the energy consumption of up exchange process, down exchange process are 0.178 MJ, 0.148 MJ, respectively.

5 Results and discussion

5.1 Model validation

Table 8 shows the comparison between estimated and measured energy consumption of test 1 and test 2 in ASHM process. Test 1 was designed to investigate the effect of deposition path, rapid moving path, and inflection points on the energy consumption at AM stage, while test 2 was designed to explore the influence of the AM process parameters and deposition efficiency on the total energy consumption in ASHM process. It can be noted that all of the predicted energy consumption are slightly lower than the measured energy consumption, and the error of the model for all samples is lower than 5%. The difference may be caused by the following reasons: (1) the dynamic change of power because of the fluctuation in current, (2) the peak power due to switching ON and switch OFF of machine equipment such as spindle or fans running are not included [37], (3) errors in the fitted model of power consumption and process parameters are always exist, (4) the effect of acceleration and deceleration of the inflection point on time is not considered during AM process, and (5) Z-axis energy consumption is neglected because the feed speed is almost zero. It also can be seen that the scanning strategy has little effect on the energy consumption in test 1. This is due to the trade-off between the length of the deposition path and the number of inflection points under different scanning strategies. For example, in the scanning strategies of D3 and D4, the length of the deposition path increases from 43,392 to 46,080 mm, while the inflection points decreases from 2320 to 1200 (Table 5). Therefore, the proportion of the deposition energy consumption increases from 80.99 to 88.87%, while the proportion of the pause energy consumption decreases from 13.87 to 7.42% (i.e., the breakdown analysis in Fig. 10), and the total energy consumption total energy consumption remains almost unchanged (Table 8).

Table 5 The data of deposition path, rapid moving path and inflection point of the four scanning strategies

Scanning strategies	Deposition path (mm)	Rapid moving path (mm)	Inflection points
D1	43,200	1417	2400
D2	43,200	2739	2400
D3	43,392	2949	2320
D4	46,080	2066	1200

On the contrary, the scanning speed has an important influence on energy consumption at AM stage. When the scanning speed increases from 500 to 1100 mm/min, the total energy consumption decreases from 42 to 29 MJ, almost 31% reduction. This is due to the increased scanning speed, which greatly increases the process rate of the deposition process (i.e., the process rate increased from 0.96 to 2.11 g/min, as listed in Table 4), resulting in lower deposition time. The decreased deposition time greatly reduces the standby energy consumption due to the high standby power of the ASHM system (i.e., the total standby power of the ASHM devices is almost 4000 W in Table 6). Even though the increase in laser power (i.e., from 500 to 1100 W) leads to an increase in energy consumption per unit time of the laser machine, the total energy consumption of the laser machine, as well as the machine tool, powder feeder, and chiller, is reduced due to the decreased deposition time. These combined reasons contribute to the energy-savings when the scanning speed is increased.

Table 9 shows the comparison between estimated and measured energy consumption of test 1 at AM stage without considering pause energy consumption. Obviously, the error of the model is more than 14% for the D1–D3 samples and 8% for the D4 sample, respectively. This is due to the time

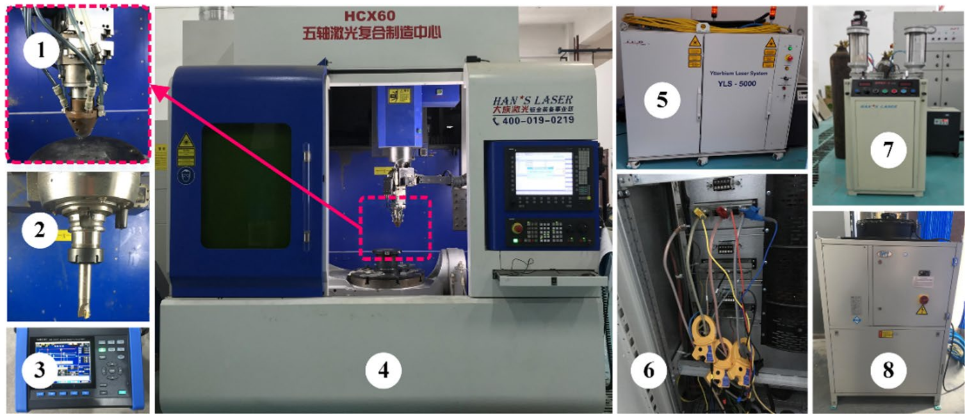

Fig. 5 Experimental apparatus (**1**: cladding head; **2**: cutting tool; **3**: HIOKI power analyzer; **4**: machine tool; **5**: laser machine; **6**: bus; **7**: powder feeder; **8**: laser chiller)

consumed by the cladding head being at the pause state. For example, the sample D1 has 2400 inflection points (as listed in Table 5), which means that the cladding head stopped 2400 times and spent 16 min, accounting for 19.64% of the total time. The time spent in pause state consumes a lot of standby energy consumption. The experimental results show that considering the pause energy consumption at AM stage can greatly improve the prediction accuracy of the energy consumption model.

5.2 Model comparison at AM stage

As mentioned in literature review, At AM stage, the SPE with the fixed value was usually adopted for life cycle assessment of the environmental impact. Recently, Lunetto et al. [38] purposed an empirical SPE model associated with process rate for predicting the energy consumption of fused deposition modeling (FDM) process, as presented in Eq. (10).

$$SPE = C_0 + \frac{C_1}{PR} \tag{10}$$

where the *SPE* is the specific printing energy in MJ/kg, *PR* is the process rate in g/min, and the C_0 and C_1 are the relevant coefficients.

The two types of SPE model, together with the state-based model purposed by this work, were used for energy consumption prediction. The average SPE of 263 MJ/kg was obtained from the energy consumption data of our 8 samples (i.e., sample of D1–D4 plus S1–S4), and the C_0 of 126.85, along with the C_1 of 174.95, was obtained through fitting the D1 to D4 enegy consumption data. The comparison results are shown in Table 10. It can be seen that the prediction accuracy of the SPE-based model fluctuates with different scanning strategies and process parameters, while the state-based model has the highest stability. Its prediction accuracy exceeds 97%. In addition, the prediction accuracy is improved by 12.87% when considering the pause energy consumption, which proved that the pause energy consumption plays an important role in the prediction accuracy of the model. The comparison results have demonstrated the effectiveness of the proposed model.

Table 6 The constant power of machines

Items	Symbols	Power (W)
Standby power of machine tool	$P_{standby\_machine\ tool}$	1879
Standby power of laser machine	$P_{standby\_laser\ machine}$	562
Standby power of laser chiller	$P_{standby\_laser\ chiller}$	1500
Standby power of powder feeder	$P_{standby\_powder\ feeder}$	~5
Axis fast movement of machine tool	P_{fast_feed}	1250
Working power of laser chiller	$P_{working\_chiller}$	4071

5.3 Energy consumption of SM stage related to deposition efficiency

Figure 7 shows the effect of deposition efficiency on SM energy consumption. It can be seen that the SM energy consumption increases with the decrease of deposition efficiency. When the deposition efficiency is increased by 7%, the SM energy consumption is reduced by 3.56 MJ in this test. Therefore, the impact of deposition efficiency on energy consumption cannot be ignored, especially for parts with complex features, which means more materials need to be removed and more associated energy need to be consumed.

5.4 Breakdown analysis and energy-saving suggestions

Figure 8 shows the distribution of energy consumption for the three sub-processes. It is obvious that the AM stage consumes most of the energy and accounts for more than 80%. This is due to the long deposition time and high

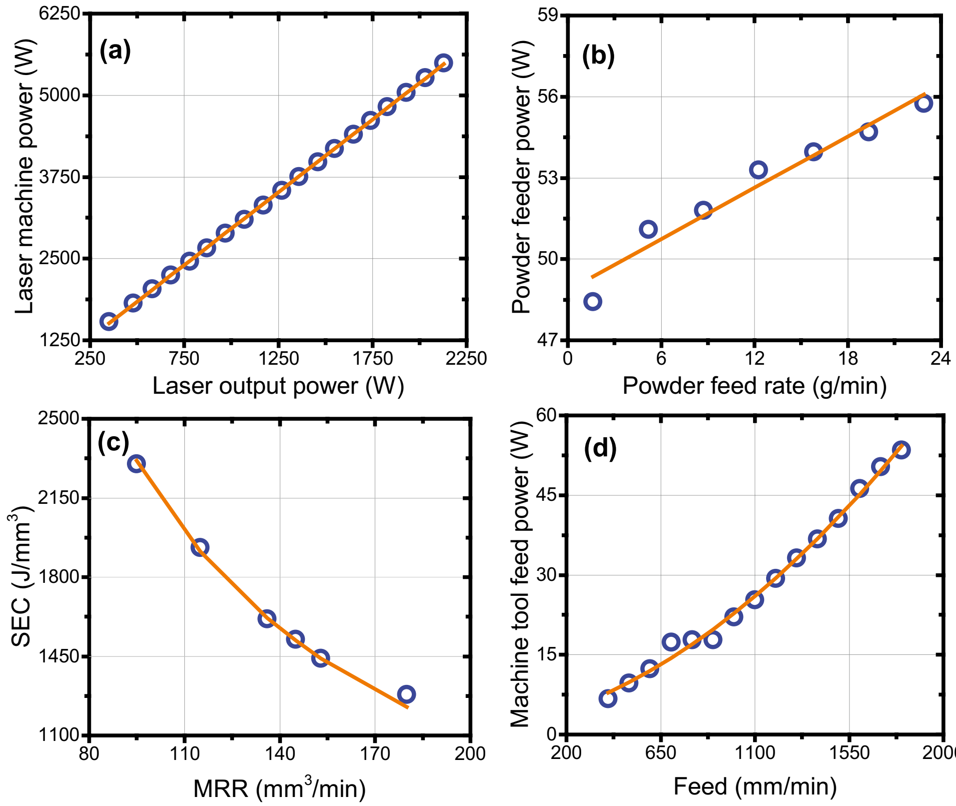

Fig. 6 Power of several devices vs process parameters

operating power. At AM stage, all the equipment such as laser machine, chiller, and machine tool must be running to achieve the near-net shape of the part. The SM process is used to remove the redundant materials of the AM parts, so that the surface of the parts can be smooth to meet the practical requirements. It can be seen that the energy consumption of SM process accounts for 8–15% during milling process of four samples. The energy consumption of exchange process are less than 1%, because in this experimental study, the exchange process only occurs once. However, we cannot ignore the energy consumption of exchange process in actual ASHM. As presented in Fig. 1, a complex part needs multiple times of AM and SM process; thus, there must be multiple exchange processes involved. It can be inferred that the more complex of parts, the larger proportion of energy consumption of exchange process will be.

The energy requirements for each equipment of the four samples in test 2 are shown in Fig. 9. Surprisingly, the laser chiller consumes a massive energy. Its energy consumption even exceeds the laser machine and accounts for more than 36%. The laser chiller is used as an auxiliary device to cool the laser machine and the cladding head. Its huge energy consumption means that the effective energy used for deposition process is relatively low. The energy requirements results suggested that increasing scanning speed could reduce the energy consumption proportion of laser chiller and improve the energy efficiency in ASHM. The laser machine consumes less energy than laser machine; however, with the scanning speed increases, its proportion will gradually increase, even exceeding the laser chiller. The powder feeder consumes the minimum energy, no more than 1% for all four samples.

Figure 10 shows the distribution of energy consumption of the three cladding head moving states at AM stage. It can be seen that different scanning strategies will lead to changes in the proportion of energy consumption in each cladding head moving state. The deposition energy consumption accounts for more than 80% of the entire AM energy consumption. However, the energy consumption in

Table 7 The specific fitting relation formula of process parameters and power consumption

Items	Symbols	Fitting formula	R^2
Working power of laser machine	$P_{working\_laser}$	$P_{working\_laser} = 729.5 + 2.2 \cdot P_{output}$	0.999
Power of powder feeder	P_{powder}	$P_{powder} = 48.9 + 0.3 \cdot v_f$	0.951
Axis feed power of machine tool	P_{feed}	$P_{feed} = 2.03 + 0.01 \cdot v_s + 1.03 \times 10^{-5} \cdot v_s^2$	0.994
SEC at SM stage	SEC	$SEC = 12.2 + \frac{218674.6}{MRR}$	0.930

Table 8 Summary of the measured and predicted energy consumption for manufacturing the 316L parts in ASHM

Tests	Samples	Measured energy (MJ)				Predicted energy (MJ)				Error[a] (%)
		AM stage	SM stage	Exchange stage	Total	AM stage	SM stage	Exchange stage	Total	
Test 1	D1	28.71	-	-	28.71	28.12	-	-	28.12	2.06
	D2	28.80	-	-	28.80	28.68	-	-	28.68	0.42
	D3	29.05	-	-	29.05	28.85	-	-	28.85	0.69
	D4	28.24	-	-	28.24	27.92	-	-	27.92	1.13
Test 2	S1	38.03	3.46	0.15	41.64	37.82	3.44	0.15	41.41	0.55
	S2	31.86	4.11	0.14	36.11	31.68	4.04	0.15	35.87	0.66
	S3	28.04	4.60	0.15	32.79	27.81	4.47	0.15	32.43	1.10
	S4	24.29	4.60	0.15	29.04	23.99	4.47	0.15	28.61	1.48

[a]Error = |total predicted value – total measured value|/ total measured value × 100%

Table 9 Comparison between estimated and measured energy consumption of AM stage without considering pause energy consumption

Tests	Samples	Measured energy at AM stage (MJ)	Predicted energy at AM stage without considering pause energy consumption (MJ)	Error[a] (%)
Test 1	D1	28.71	23.98	16.48
	D2	28.80	24.64	14.43
	D3	29.05	24.85	14.47
	D4	28.24	25.85	8.46

[a]Error = |predicted value – measured value|/ measured value × 100%

Table 10 Comparison of the predicted and measured energy consumption at AM stage

Models	SPE (MJ/kg)	Predicted energy consumption (MJ)				Error[a] (%)					Accuracy[b] (%)
		D1	D4	S1	S4	D1	D4	S1	S4	Average	
①	263	23.67	23.67	23.67	23.67	17.54	16.19	34.56	0.72	17.25	82.75
②	-	23.00	23.00	26.41	21.84	18.22	17.66	25.68	4.53	16.52	83.48
③[c]	-	23.98	25.85	31.61	18.31	16.48	8.47	12.61	22.08	14.91	85.09
This work	-	28.12	27.92	35.53	22.88	3.10	2.15	1.79	2.71	2.44	97.56

[a]Error = (|predicted value – measured value|/measured value) × 100%

[b]Accuracy = 100 – Error

[c]The energy consumption model at AM stage without considering pause energy consumption in this work

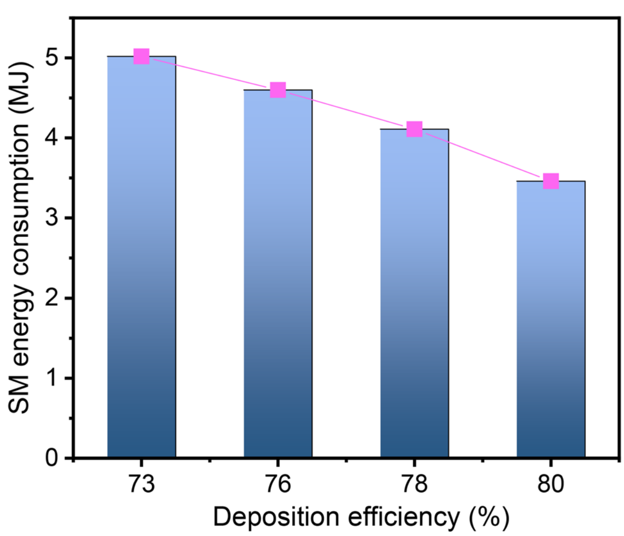

Fig. 7 The SM energy consumption vs deposition efficiency

rapid moving state and pause state cannot be ignored. The number of inflection points and the length of the rapid moving path should be minimized when the scanning strategy of the printed part is planned.

Through the research on ASHM process, this work has shown that the scanning speed has an important impact on energy consumption. The increasing scanning speed could greatly improve the process rate and shorten the deposition time during AM process. The example of manufacturing the simplified aviation bearing seat by ASHM process is illustrated in Fig. 11. When the process rate is increased from 0.34 to 3.13 g/min by changing the scanning speed, the total ASHM energy consumption is reduced from 2013 to 221 MJ, an 89% reduction. This is due to the increased process rate reduces the deposition time, thereby greatly reducing the standby energy consumption of multiple energy-consuming devices of the ASHM system. However, the

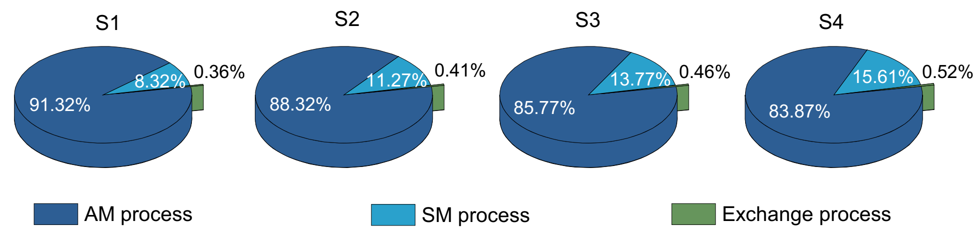

Fig. 8 The distribution of energy consumption of AM process, SM process and exchange process

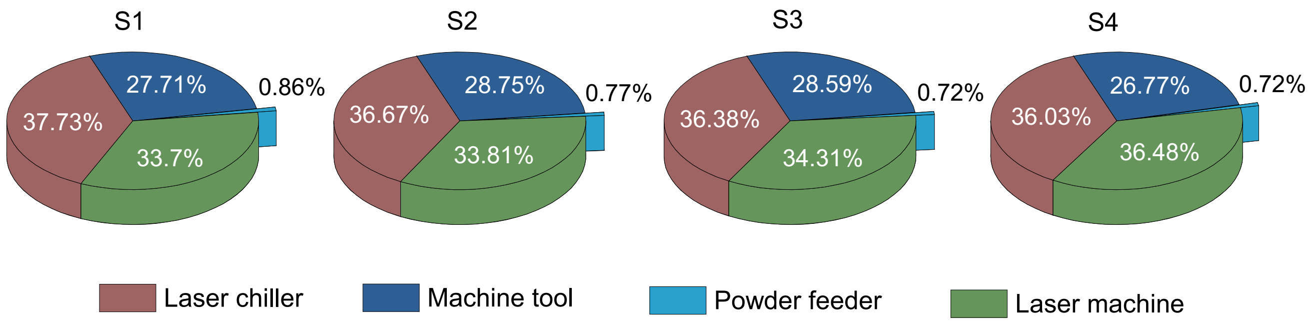

Fig. 9 The energy requirements of each machine in ASHM

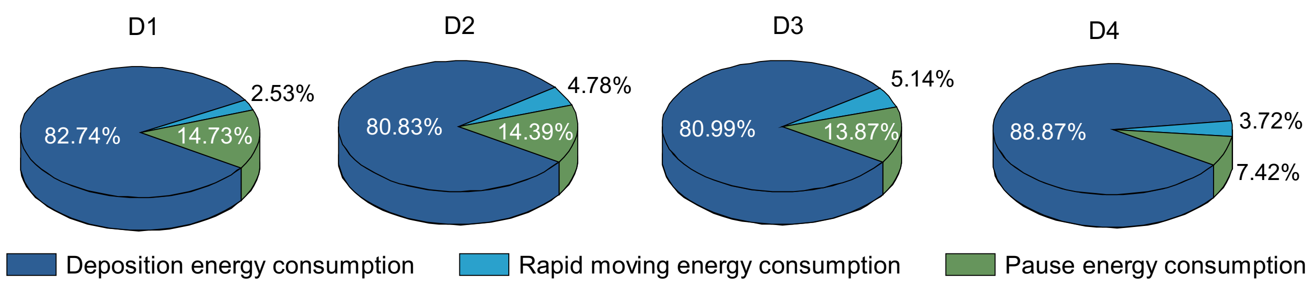

Fig. 10 The distribution of energy consumption of the three cladding head moving states at AM stage

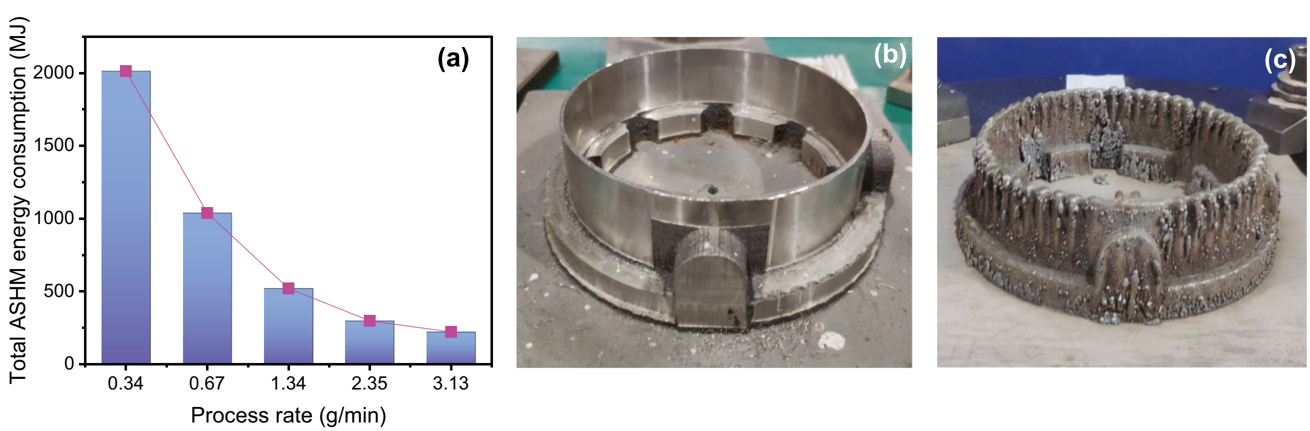

Fig. 11 The simplified aviation bearing seat manufactured by ASHM process with the 70% deposition efficiency: (**a**) the energy consumption vs process rate; (**b**) the deposited part after milling; (**c**) the deposited condition with excessive scanning speed

scanning speed cannot be increased indefinitely. As verified by our experiments, excessive scanning speed can reduce the forming quality of parts, such as collapse (Fig. 11c). This is due to the fact that the excessive scanning speed will cause the melt pool to become unstable, and the unstable melt pool is unable to melt the ejected powder uniformly, thus failing to form the stable deposition tracks. Multiple track-to-track overlap and layer-to-layer accumulation will eventually cause the collapse of the edge of the deposited part. In addition, according to the breakdown analysis, the chiller machine consumes a lot of energy. It is recommended to choose cooling equipment with lower rated power on the premise of meeting the cooling requirements to reduce its standby energy consumption.

6 Conclusions

The ASHM process consumes a significant amount of electrical energy due to the multiple power-consuming equipment and various operating states, which results in substantial stress on the environment. Understanding the energy consumption characteristics can provide the basis for energy-saving. In this paper, a methodology to predict the energy consumption in ASHM process was presented. The following points were summarized.

1. A combined energy consumption model based on cladding head moving state and deposition efficiency was developed to predict the energy consumption of ASHM process.
2. The model was verified by two experimental studies, and the prediction accuracy exceeds 97%.
3. The energy consumption of AM stage accounts for more than 80% of the total ASHM energy consumption due to the long deposition time and high operating power.
4. It is recommended to increase the scanning speed under the premise of ensuring the good forming quality to shorten the deposition time and reduce the energy consumption. Moreover, choosing a low-power chiller machine under the premise of ensuring the cooling requirements can effectively reduce the standby energy consumption of the ASHM process.

Author contribution Wen Liu designed and drafted the manuscript, Haiying Wei conceived the project and organized the paper, Min Zhang designed the verification method, Yaoen Luo performed the experiments and recorded the data, Wen Liu and Min Zhang analyzed the data, and Yi Zhang contributed to overall evaluation and revised the paper. All authors read and approved the manuscript.

Funding This work was supported by National Natural Science Foundation of China (Grant No. 51975205) and the Natural Science Foundation of Hunan Province, China (Grant No. 2020JJ4202). Their financial contributions are gratefully acknowledged.

Data availability All data needed to evaluate the conclusions in the paper are present. Additional data related to this paper are available from the corresponding authors upon reasonable requests.

Declarations

Ethics approval Not applicable.

Consent to participate All the participated persons are listed in the article or acknowledged in the paper.

Consent for publication The authors consent to transfer the copyright of the article to publish.

Conflict of interest The authors declare no competing interests.

References

1. Flynn JM, Shokrani A, Newman ST, Dhokia V (2016) Hybrid additive and subtractive machine tools – research and industrial developments. Int J Mach Tool Manu 101:79–101. https://doi.org/10.1016/j.ijmachtools.2015.11.007
2. Jackson MA, Van AA, Morrow JD, Min S, Pfefferkorn FE (2018) Energy consumption model for additive-subtractive manufacturing processes with case study. Int J Pr Eng Man-Gt 5:459–466. https://doi.org/10.1007/s40684-018-0049-y
3. Soshi M, Ring J, Young C, Oda Y, Mori M (2017) Innovative grid molding and cooling using an additive and subtractive hybrid CNC machine tool. CIRP Ann-Manuf Techn 66:401–404. https://doi.org/10.1016/j.cirp.2017.04.093
4. Oyesola MO, Mpofu K, Mathe NR, Daniyan IA (2020) Hybrid-additive manufacturing cost model: a sustainable through-life engineering support for maintenance repair overhaul in the aerospace. Procedia Manuf 49:199–205. https://doi.org/10.1016/j.promfg.2020.07.019
5. Peng S, Li T, Wang X, Dong M, Liu Z, Shi J, Zhang H (2017) Toward a sustainable impeller production: Environmental impact comparison of different impeller manufacturing methods. J Ind Ecol 21:S216–S229. https://doi.org/10.1111/jiec.12628
6. Li P, Gong Y, Liang C, Yang Y, Cai M (2019) Effect of post-heat treatment on residual stress and tensile strength of hybrid additive and subtractive manufacturing. Int J Adv Manuf Tech 103:2579–2592. https://doi.org/10.1007/s00170-019-03705-2
7. Yang Y, Gong Y, Qu S, Xie H, Cai M, Xu Y (2020) Densification, mechanical behaviors, and machining characteristics of 316L stainless steel in hybrid additive/subtractive manufacturing. Int J Adv Manuf Tech 107:177–189. https://doi.org/10.1007/s00170-020-05033-2
8. Gutowski T, Jiang S, Cooper D, Corman G, Hausmann M, Manson JA, Schudeleit T, Wegener K, Sabelle M, Ramos GJ, Sekulic DP (2017) Note on the rate and energy efficiency limits for additive manufacturing. J Ind Ecol 21:S69–S79. https://doi.org/10.1111/jiec.12664
9. Kellens K, Mertens R, Paraskevas D, Dewulf W, Duflou JR (2017) Environmental impact of additive manufacturing processes: does AM contribute to a more sustainable way of part manufacturing.

Procedia CIRP 61:582–587. https://doi.org/10.1016/j.procir.2016.11.153

10. Yoon HS, Singh E, Min S (2018) Empirical power consumption model for rotational axes in machine tools. J Clean Prod 196:370–381. https://doi.org/10.1016/j.jclepro.2018.06.028
11. Yang S, Min W, Ghibaudo J, Zhao YF (2019) Understanding the sustainability potential of part consolidation design supported by additive manufacturing. J Clean Prod 232:722–738. https://doi.org/10.1016/j.jclepro.2019.05.380
12. Ingarao G, Priarone PC, Deng Y, Paraskevas D (2018) Environmental modelling of aluminium based components manufacturing routes: additive manufacturing versus machining versus forming. J Clean Prod 176:261–275. https://doi.org/10.1016/j.jclepro.2017.12.115
13. Priarone PC, Ingarao G (2017) Towards criteria for sustainable process selection: on the modelling of pure subtractive versus additive/subtractive integrated manufacturing approaches. J Clean Prod 144:57–68. https://doi.org/10.1016/j.jclepro.2016.12.165
14. Liu ZY, Li C, Fang XY, Guo YB (2018) Energy consumption in additive manufacturing of metal parts. Procedia Manuf 26:834–845. https://doi.org/10.1016/j.promfg.2018.07.104
15. Peng T, Chen C (2018) Influence of energy density on energy demand and porosity of 316L stainless steel fabricated by selective laser melting. Int J Pr Eng Man-Gt 5:55–62. https://doi.org/10.1007/s40684-018-0006-9
16. Lv J, Peng T, Zhang Y, Wang Y (2020) A novel method to forecast energy consumption of selective laser melting processes. Int J Prod Res 59:1–17. https://doi.org/10.1080/00207543.2020.1733126
17. Feng M, Hua Z, Hon KKB, Qingshan G (2018) An optimization approach of selective laser sintering considering energy consumption and material cost. J Clean Prod 199:529–537. https://doi.org/10.1016/j.jclepro.2018.07.185
18. Zhu Y, Peng T, Jia G, Zhang H, Xu S, Yang H (2019) Electrical energy consumption and mechanical properties of selective-laser-melting-produced 316L stainless steel samples using various processing parameters. J Clean Prod 208:77–85. https://doi.org/10.1016/j.jclepro.2018.10.109
19. Shamsaei N, Yadollahi A, Bian L, Thompson SM (2015) An overview of direct laser deposition for additive manufacturing Part II: Mechanical behavior, process parameter optimization and control. Addit Manuf 8:12–35. https://doi.org/10.1016/j.addma.2015.07.002
20. Jin Y, He Y, Fu G, Zhang A, Du J (2017) A non-retraction path planning approach for extrusion-based additive manufacturing. Robot CIM-Int Manuf 48:132–144. https://doi.org/10.1016/j.rcim.2017.03.008
21. Volpato N, Galvao LC, Nunes LF, Souza RI, Oguido K (2020) Combining heuristics for tool-path optimisation in material extrusion additive manufacturing. J Oper Res Soc 71:867–877. https://doi.org/10.1080/01605682.2019.1590135
22. Weller TR, Weller DR, Rodrigues LC, Volpato N (2021) A framework for tool-path airtime optimization in material extrusion additive manufacturing. Robot CIM-Int Manuf 67:101999. https://doi.org/10.1016/j.rcim.2020.101999
23. Wang J, Lin X, Li J, Hu Y, Zhou Y, Wang C, Li Q, Huang W (2019) Effects of deposition strategies on macro/microstructure and mechanical properties of wire and arc additive manufactured Ti 6Al 4V. Mat Sci Eng A-Struct 754:735–749. https://doi.org/10.1016/j.msea.2019.03.001
24. Habib MA, Khoda B (2017) Attribute driven process architecture for additive manufacturing. Robot CIM-Int Manuf 44:253–265. https://doi.org/10.1016/j.rcim.2016.10.003
25. Komineas G, Foteinopoulos P, Papacharalampopoulos A, Stavropoulos P (2018) Build time estimation models in thermal extrusion additive manufacturing processes. Procedia Manuf 21:647–654. https://doi.org/10.1016/j.promfg.2018.02.167
26. Hedrick RW, Urbanic RJ, Burford CG (2015) Development considerations for an additive manufacturing CAM system. IFAC-PO 48:2327–2332. https://doi.org/10.1016/j.ifacol.2015.06.435
27. Chen L, Xu K, Tang K (2018) Optimized sequence planning for multi-axis hybrid machining of complex geometries. Comput Graph 70:176–187. https://doi.org/10.1016/j.cag.2017.07.018
28. Chen X, Li C, Jin Y, Li L (2018) Optimization of cutting parameters with a sustainable consideration of electrical energy and embodied energy of materials. Int J Adv Manuf Tech 96:775–788. https://doi.org/10.1007/s00170-018-1647-0
29. Li L, Huang HH, Zou X, Zhao F, Li GS, Liu ZF (2021) An energy-efficient service-oriented energy supplying system and control for multi-machine in the production line. Appl Energ 286:116483. https://doi.org/10.1016/j.apenergy.2021.116483
30. Cao HJ, Zhou J, Jiang P, Hon KKB, Yi H, Dong CY (2020) An integrated processing energy modeling and optimization of automated robotic polishing system. Robot CIM-Int Manuf 65:101973. https://doi.org/10.1016/j.rcim.2020.101973
31. Jin YA, He Y, Fu JZ, Gan WF, Lin ZW (2014) Optimization of tool-path generation for material extrusion-based additive manufacturing technology. Addit Manuf 1:32–47. https://doi.org/10.1016/j.addma.2014.08.004
32. Sun YW, Jia JJ, Xu JT, Chen M, Niu JB (2021) Path, feedrate and trajectory planning for free-from surface machining: a state-of-the-art review. Chinese J Aeronaut. https://doi.org/10.1016/j.cja.2021.06.011
33. Castelino K, D'Souza R, Wright PK (2003) Toolpath optimization for minimizing airtime during machining. J Manuf Syst 22:173–180. https://doi.org/10.1016/S0278-6125(03)90018-5
34. Rico GH, Sanchez RJL, Gomis HM, Rao RV (2020) Parallel implementation of metaheuristics for optimizing tool path computation on CNC machining. Comput Ind 123:103322. https://doi.org/10.1016/j.compind.2020.103322
35. Yang D, He C, Zhang G (2016) Forming characteristics of thin-wall steel parts by double electrode GMAW based additive manufacturing. J Mater Process Tech 227:153–160. https://doi.org/10.1016/j.jmatprotec.2015.08.021
36. Kara S, Li W (2011) Unit process energy consumption models for material removal processes. CIRP Ann-Manuf Techn 60:37–40. https://doi.org/10.1016/j.cirp.2011.03.018
37. Aramcharoen A, Mativenga PT (2014) Critical factors in energy demand modelling for CNC milling and impact of toolpath strategy. J Clean Prod 78:63–74. https://doi.org/10.1016/j.jclepro.2014.04.065
38. Lunetto V, Priarone PC, Galati M, Minetola P (2020) On the correlation between process parameters and specific energy consumption in fused deposition modelling. J Manuf Process 56:1039–1049. https://doi.org/10.1016/j.jmapro.2020.06.002